Macrophages Induce Long-Term Trapping of $\gamma\delta$ T Cells with Innate-like Properties within Secondary Lymphoid Organs in the Steady State

Alexandra Audemard-Verger, Matthieu Rivière, Aurélie Durand, Elisa Peranzoni, Vincent Guichard, Pauline Hamon, Nelly Bonilla, Thomas Guilbert, Alexandre Boissonnas, Cédric Auffray, et al.

Macrophages induce long-term trapping of γδ T cells with innate-like properties within secondary lymphoid organs in the steady state

By

Alexandra Audemard-Verger[1*], Matthieu Rivière[1*], Aurélie Durand[1*], Elisa Peranzoni[1], Vincent Guichard[1,2], Pauline Hamon[3], Nelly Bonilla[1], Thomas Guilbert[1], Alexandre Boissonnas[3], Cédric Auffray[1], Gérard Eberl[4], Bruno Lucas[1**] and Bruno Martin[1**]

[1] Paris Descartes Université, Institut Cochin, CNRS UMR8104, INSERM U1016, 75014 Paris, France; [2] Paris Diderot Université; [3] Sorbonne Universités, UPMC Université Paris 06, INSERM U1135, CNRS ERL8255, Centre d'Immunologie et des Maladies Infectieuses, 91 Boulevard de l'Hôpital, 75013 Paris, France; [4] Unité Microenvironment & Immunity, Institut Pasteur, 75724 Paris, France, INSERM U1224, 75724 Paris, France.

[*] Alexandra Audemard-Verger, Matthieu Rivière and Aurélie Durand contributed equally to this paper.

[**] Bruno Lucas and Bruno Martin contributed equally to this paper.

Corresponding author: Dr. Bruno Martin (bruno.martin@inserm.fr), Cochin Institute, 75014 Paris, France. Phone: 33-1-40516589; Fax: 33-1-40516535

Running title: γδ T-cell residency in secondary lymphoid organs

Keywords: Gamma delta T cells; Secondary lymphoid organs; T-cell trafficking; Steady state

ABSTRACT

So far, peripheral T cells are mostly described to circulate between blood, secondary lymphoid organs and lymph in the steady state. This nomadic existence would allow them to accomplish their surveying task for both foreign antigens and survival signals. Although it is now well established that γδ T cells can be rapidly recruited to inflammatory sites or in certain tumor microenvironments, the trafficking properties of peripheral γδ T cells have been poorly studied in the steady state. In the present paper, we highlight the existence of resident γδ T cells in the secondary lymphoid organs of specific pathogen free mice. Indeed, using several experimental approaches such as the injection of integrin-neutralizing antibodies which inhibit the entry of circulating lymphocytes into lymph nodes and long-term parabiosis experiments, we have found that, contrary to Ly6C$^{-/+}$ CD44^{lo} and Ly-6C^{+} CD44^{hi} γδ T cells, a significant proportion of Ly-6C^{-} CD44^{hi} γδ T cells are trapped for long periods of time within lymph nodes and the spleen in the steady state. Specific *in vivo* cell-depletion strategies have allowed us to demonstrate that macrophages are the main actors involved in this long-term retention of Ly-6C^{-} CD44^{hi} γδ T cells in secondary lymphoid organs.

INTRODUCTION

γδ T cells are unique and distinct from other lymphocyte subsets, such as NK cells, B cells, and αβ T cells, in that they combine adaptive features with rapid, innate-like responses that allow them to play an important role in all phases of an immune response. γδ T cells are crucially involved in host immune defense against infections (1) but are also known to have a strong clinical association with various autoimmune diseases such as inflammatory bowel disease (2, 3), rheumatoid arthritis (or collagen-induced arthritis, the murine model of rheumatoid arthritis) (4, 5), and multiple sclerosis (or experimental autoimmune encephalomyelitis, the murine model of multiple sclerosis) (6, 7).

In addition, there is compelling evidence to indicate that γδ T cells play an important role in immunity to cancer by sensing and reacting to cellular stress. This has been clearly demonstrated in murine models of spontaneous (8), chemically induced (9), transgenic (10), and transplantable tumors (11, 12). However, it seems that the activity of γδ T cells in response to tumors can differ radically according to the tumor type or environment (13, 14). These data may actually reflect the high diversity of the γδ T cell compartment.

In this regard, we have recently showed that within murine secondary lymphoid organs (SLOs), γδ T cells can be subdivided into four subsets according to CD44 and Ly-6C expression. More precisely, we have characterized the functional heterogeneity of the peripheral γδ T cell compartment that comprises Ly-6C^{-} CD44^{hi} γδ T cells exhibiting innate-like features and naive and memory adaptive-like γδ T cells (Ly6C$^{-/+}$ CD44^{lo} γδ T cells and Ly-6C^{+} CD44^{hi} γδ T cells respectively; (15)).

This phenotypic and functional heterogeneity of the peripheral γδ T-cell compartment may be also associated with differential T-cell trafficking dynamic properties. So far, peripheral T

67 cells are mostly described to circulate between blood, SLOs and lymph in the steady state.
68 This nomadic existence would allow them to accomplish their surveying task for both foreign
69 antigens and survival signals (16, 17). In line with this concept, Mandl et al., have showed in
70 a recent study that the mean transit time for $CD4^+$ and $CD8^+$ αβ T cells in peripheral lymph
71 nodes (pLNs) were of 12 and 18 hours respectively (18). Concerning γδ T cells, it is now well
72 established that γδ T cells can be rapidly recruited to inflammatory sites or to certain tumor
73 microenvironments (19, 20). These γδ T-cell infiltrations are notably orchestrated by
74 inflammatory cytokines such as IL-1β or IL-23 or chemokine axes such as CCL2/CCR2 (12,
75 21, 22, 23). However, the T-cell trafficking dynamics of peripheral γδ T-cell subsets in the
76 steady state have still been poorly studied.

77 Here, using several experimental approaches such as the injection of integrin-neutralizing
78 antibodies which inhibit the entry of circulating lymphocytes into lymph nodes (LNs) and
79 long-term parabiosis experiments, we have found that contrary to Ly-$6C^+$ $CD44^{hi}$ and $CD44^{lo}$
80 γδ T-cell subsets which are circulating cells, an important proportion of Ly-$6C^-$ $CD44^{hi}$ γδ T
81 cells is residing within SLOs in the steady state. Moreover, specific *in vivo* cell-depletion
82 strategies have allowed us to demonstrate that macrophages are the main actors involved in
83 this long-term trapping of Ly-$6C^-$ $CD44^{hi}$ γδ T cells in SLOs in the steady state.

MATERIALS AND METHODS

Mice

C57BL/6 CD45.1 mice, C57BL/6 CD45.2 mice, C57BL/6 μMT mice and C57BL/6 CD11c.DTR mice (24), were maintained in our own animal facilities, under specific pathogen-free conditions. C57BL/6 RORγt-GFP mice were initially obtained from Dr. Gerard Eberl, Institut Pasteur, France (25). 6- to 12-week-old mice were used for experiments. Animal housing, care and research were carried out in accordance with the guidelines of the French Veterinary Department. All procedures were approved by the French animal experimentation and ethics committee and validated by "Service Protection et Santé Animales, Environnement" with the numbers C-75-562 and A-75-1315. Sample sizes were chosen to assure reproducibility of the experiments and in accordance with the 3R of animal ethics regulation.

Cell suspensions

Peripheral lymph nodes (pooled cervical, axillary, brachial and inguinal lymph nodes; pLNs), mesenteric LNs (mLNs), cervical LNs (cLNs), and spleen were homogenized and passed through a nylon cell strainer (BD Falcon) in RPMI 1640 Glutamax (Gibco) supplemented with 10% fetal calf serum (FCS; Biochrom) for adoptive transfer and cell culture (LNs only), or in 5% FCS, 0.1% NaN3 (Sigma-Aldrich) in phosphate saline buffer saline (PBS), for flow cytometry.

To verify the efficiency of DCs or macrophages *in vivo* depletion, LNs and Spleens were disrupted in RPMI medium containing 5% FCS, 1 mg Collagenase from Clostridium histolyticum type II and type IV (Sigma) and 0.5 mg DNase I (Sigma) and incubated for 20 min at 37 °C.

Fluorescence staining and flow cytometry

111 Cell suspensions were collected and dispensed into 96-well round-bottom microtiter plates
112 (Greiner Bioscience; $6x10^6$ cells/well). Surface staining was performed as previously
113 described (26, 27). Briefly, cells were incubated on ice, for 15 minutes per step, with
114 antibodies (Abs) in 5% FCS (Biochrom), 0.1% NaN_3 (Sigma-Aldrich) PBS. Each cell-staining
115 reaction was preceded by a 15-minute incubation with a purified anti-mouse CD16/32 Ab
116 (FcγRII/III block; 2.4G2) obtained from hybridoma supernatants. For determination of
117 intracellular cytokine production, cells were stimulated with 0.5 μg/ml PMA (Sigma-
118 Aldrich), 0.5 μg/ml ionomycin (Sigma-Aldrich), and 10 μg/ml BrefeldinA (Sigma-Aldrich)
119 for 2 hours at 37°C. Cells were then stained for surface markers, fixed in 2%
120 paraformaldehyde in PBS, and permeabilized with 0.5% saponin, followed by labeling with
121 specific cytokine Abs.
122 S1PR1 was detected with a rat monoclonal antibody (R&D Systems). Briefly, cells were first
123 incubated for 90 min with the anti-S1PR1 rat mAb (50μg/ml) in PBS containing 0.5% FCS,
124 1mM EDTA, 0.05% azide and 2% normal mouse serum. After washing, cells were then
125 incubated with donkey biotinylated anti–rat IgG polyclonal Abs (Jackson ImmunoReaserch)
126 for 30 min in the above medium followed by streptavidin-APC (BioLegend).
127 Multicolor immunofluorescence was analyzed using BD LSR2 and BD Fortessa cytometers
128 (BD Biosciences). List-mode data files were analyzed using Diva software (BD Biosciences).
129 Data acquisition was performed on the Cochin Cytometry and Immunobiology (CIBIO)
130 facility.
131 **Parabiosis**
132 Female host parabionts were generated with 8-12 week-old C57BL/6 CD45.1 mice and
133 C57BL/6 CD45.2 mice. The percentage of host cells in a given T-cell subset corresponds to
134 the percentage of $CD45.1^+$ cells for the CD45.1 parabiont and the percentage of $CD45.2^+$ cells
135 for the CD45.2 parabiont.

Blocking T-cell entry into LNs

Purified anti-VLA-4 (α4) (clone PS/2) and anti-LFA-1 (αL) (clone M17/4) Abs were obtained from Bio-XCell. For short-term treatment, mice were injected intraperitoneally one time with 200μg of both Abs and then analyzed 48 hours later. For long-term treatment, mice were injected intraperitoneally every 2 days during 6 days (4 injections) with 200μg of both Abs and analyzed 24 hours later.

***In vivo* cell depletions**

For dendritic cell depletion, C57BL/6 CD11c.DTR mice (referred as CD11c DOG mice) were injected intraperitoneally every 2 days during 6 days (4 injections) with 250ng of Diphtheria Toxin (DT).

The CSF1R inhibitor PLX3397 incorporated into rodent chow at 290 p.p.m. (delivering daily doses of approximately 45 mg kg^{-1}) was provided along with control chow from Plexxikon Inc. (Berkeley, CA). For macrophage *in vivo* depletion, C57BL/6 mice were fed with PLX3397 or control chow during 7 days.

FTY720 treatment

Mice were injected intraperitoneally daily with FTY720 (Cayman Chemical) in saline at a dose of ~1μg/g during 7 days.

Immunofluorescence microscopy

Inguinal, axillary, brachial and maxillary mouse LNs were initially fixed overnight in 0.1M phosphate buffer containing 75mM L-Lysine, 10mM NaIO4 and 1% PFA (PLP fixative buffer). These organs were then embedded in 5% low-gelling-temperature agarose (type VII-A; Sigma-Aldrich) prepared in PBS. 230-μm LN-slices were cut with a vibratome (VT 1000S; Leica) in a bath of ice-cold PBS. Slices were then incubated at 37°C, for 20 minutes per step, with Abs in PBS. Stained slices were photographed on an upright Leica stand with a confocal spinning disk Yokogawa head with a 25x 0.95 Leica objective. Acquisitions were

made with Flash 4 LT HAMAMATSU camera. Analysis has been performed using Image J software. Data acquisition was performed on the Cochin imaging photonic (IMAG'IC) facility.

***In vivo* LPS challenge**

C57BL/6 RORγt-GFP mice were injected intravenously with 100μg of LPS (from Escherichia Coli 0111:B4; Sigma). Three hours after LPS challenge, cells recovered from pLNs, mLNs and the spleen were incubated with 10 μg/ml BrefeldinA (Sigma-Aldrich) for 2 hours at 37°C for determination of intracellular cytokine production.

Statistics

Data are expressed as mean ± SEM, and the significance of differences between two series of results was assessed using the student's paired or unpaired t test. Values of $p < 0.05$ were considered significant. (*, $p < 0.05$; **, $p < 0.01$; ***, $p < 0.001$; ****, $p < 0.0001$).

RESULTS

An important proportion of Ly-6C^{-} CD44^{hi} γδ T lymphocytes are trapped in LNs in the steady state

According to Ly-6C and CD44 expression, we have recently characterized the heterogeneity of the peripheral γδ T cell compartment by showing that it comprises Ly-6C^{-} CD44^{hi} γδ T cells exhibiting innate-like features and naive and memory adaptive-like γδ T cells (Ly6C$^{-/+}$ CD44^{lo} γδ T cells and Ly-6C^{+} CD44^{hi} γδ T cells respectively (15)). To go further, we have now decided to study the T-cell trafficking dynamics of these subsets. We first inhibited the entry of circulating lymphocytes into LNs through the injection of integrin-neutralizing antibodies (18, 28 , 29). More precisely, C57BL/6 mice were injected i.p. with anti-LFA-1 (αL) and anti-VLA-4 (α4) antibodies (Fig. 1A). We first verified that all γδ T cells from peripheral LNs, mesenteric LNs and the spleen were expressing both LFA-1 and VLA-4 integrins (Fig. S1). The phenotype of γδ T cells remaining within LNs was analyzed 48 hours after initiating the treatment (Fig. 1A). Interestingly, at that time-point, Ly-6C^{-} CD44^{hi} γδ T cells were greatly enriched within the γδ T cells remaining within peripheral LNs (pLNs; Fig. 1B-C). This resulted from the fact that the great majority of Ly-6C^{-} CD44^{hi} γδ T cells (~75%) remained trapped within pLNs whereas almost all the other γδ T cells have egressed from them (Fig. 1D). Such a phenomenon could also be observed, to a lower extent, in mesenteric LNs (mLNs) as about 15% of the Ly-6C^{-} CD44^{hi} γδ T cells were still present within this SLO 48 hours after the injection of integrin-neutralizing antibodies (Fig. 1C-D). Of note, in this model, we observed a strong increase in the absolute numbers of all the different γδ T-cell subsets in the spleen (Fig. 1D). This phenomenon could result from the accumulation in the spleen of T lymphocytes egressing from LNs.

Narayan et al. (30) have previously showed that distinct cell types in the γδ T-cell lineage

could be identified on the basis of their TCR repertoire usage. Therefore, we then analyzed the Vγ-chain repertoire of Ly-6C^{-} CD44^{hi} γδ T cells remaining within pLNs and mLNs after the injection of integrin-neutralizing antibodies (Fig. 1E). Although we noticed a decreased proportion of Vγ1.1-expressing cells associated with an enrichment of Vγ2-expressing cells within pLNs following treatment, such a discrepancy was not observed within mLNs, indicating that Vγ-chain usage does not allow to precisely identify LN-trapped γδ T lymphocytes.

Consistent with the fact that Ly-6C^{-} CD44^{hi} γδ T lymphocytes are the only γδ T cells able to produce IL-17 in response to stimulation (15), we observed, after treatment, within both peripheral and mesenteric LNs, a clear and significant increase in the proportion of IL-17-producing γδ T cells correlated with a diminished ability of the remaining γδ T cells to produce IFNγ (Fig. 1F-G).

Because circulatory dynamics could differ between γδ T-cell subsets (i.e. Ly-6C^{-} CD44^{hi} γδ T cells could need more time to exit LNs than Ly-6C^{+} CD44^{hi} and CD44^{lo} γδ T cells), we then decided to extend to 7 days the duration of the treatment blocking T-cell entry into LNs from the blood (Fig. 1H). In this setting, we still observed that whereas almost all Ly-6C^{+} CD44^{hi} and CD44^{lo} γδ T cells have left LNs, the great majority of Ly-6C^{-} CD44^{hi} γδ T cells were still trapped in pLNs and to a lesser extent in mLNs (Fig. 1I). Taken together, our data suggest that contrary to the other γδ T-cell subsets, Ly-6C^{-} CD44^{hi} γδ T lymphocytes from LNs are in part non-circulating cells.

A significant proportion of Ly-6C^{-} CD44^{hi} γδ T lymphocytes is long-term SLO-resident cells in the steady state

To explain the results presented above, one may argue that Ly-6C^{-} CD44^{hi} γδ T cells could enter into LNs in a LFA-1- and VLA-4-independent manner. To address this issue, we then

examined the cell exchange rate of the various γδ T-cell subsets from SLOs (using CD45.1 and CD45.2 congenic markers) that occurred between parabiotic pairs (Fig. 2A). Four weeks following surgery, although both Ly-6C^{+} CD44^{hi} and CD44^{lo} γδ T cells have achieved full chimerism in all studied SLOs, Ly-6C^{-} CD44^{hi} lymphocytes showed only limited exchange between the parabionts (Fig. 2B). In line with a weak circulatory dynamic of Ly-6C^{-} CD44^{hi} γδ T cells, we also observed a limited exchange of splenic IL-17-producing γδ T cells between parabiotic mice (Fig. 2C). To examine whether these results were stable over time, we performed longer-term parabiosis experiments (Fig. 2D). Eight weeks post-surgery, in all studied SLOs, Ly-6C^{-} CD44^{hi} γδ T lymphocytes still showed limited exchange between the paired mice (Fig. 2E). Altogether, these findings suggest strongly that an important proportion of Ly-6C^{-} CD44^{hi} γδ T lymphocytes corresponds to long-term SLO-resident cells in the steady state.

Macrophages are responsible for the long-term trapping of Ly-6C^{-} CD44^{hi} γδ T lymphocytes within SLOs in the steady state

We then attempted to identify the cellular actors involved in the retention of Ly-6C^{-} CD44^{hi} γδ T cells within SLOs. We first studied the potential involvement of B cells in this process. B-cell-deficient or -proficient C57BL/6 mice were treated or not with integrin-neutralizing antibodies and analyzed 48 hours later (Fig. 3A). The retention rate (recovery) of Ly-6C^{-} CD44^{hi} γδ T cells in pLNs and mLNs was comparable in both mouse strains, 48 hours after blocking T-cell entry (Fig 3B). Thus, B lymphocytes do not seem to be involved in the trapping of Ly-6C^{-} CD44^{hi} γδ T cells within LNs.

We next assessed whether dendritic cells (DCs) played a role in the retention of this γδ T-cell subset in LNs. For this purpose, C57BL/6 CD11c.DTR mice (designated CD11c.DOG), that allow, following Diphtheria Toxin (DT) injections, a continuous *in vivo* depletion of DCs,

were injected or not with anti-αL and anti-α4 antibodies (Fig. 3C). We first assessed the depletion efficiency of such a protocol (Fig. S2A-B). Depletion was quite efficient for plasmacytoid DCs in all LNs and better for the other DC subsets in mLNs than in pLNs. The recovery of Ly-6C^{-} CD44^{hi} γδ T cells in both pLNs and mLNs 48 hours after blocking T-cell entry into LNs was not diminished by DC depletion (Fig. 3D) suggesting that these latter cells are not crucially involved in the retention of Ly-6C^{-} CD44^{hi} γδ T cells within SLOs.

Finally, we examined whether macrophages could contribute to Ly-6C^{-} CD44^{hi} γδ T-cell retention within SLOs. To test this hypothesis, C57BL/6 mice were fed with mouse chow containing an inhibitor of CSF1R (PLX3397, provided by Plexxikon Inc.) for 7 days (Fig. 3E). We first assessed the depletion efficiency of such a protocol (Fig. S1C). This protocol led to the depletion of the majority of subcapsular (F4/80^{-} CD169^{+}) and medullary (F4/80^{+} CD169^{+}) sinus macrophages in both pLNs and mLNs whereas F4/80^{+} CD169^{-} macrophages were only poorly affected especially in pLNs. We found that the absolute numbers of Ly-6C^{-} CD44^{hi} γδ T cells in pLNs, mLNs and the spleen dropped dramatically in mice fed 7 days with PLX3397 chow (Fig. 3F). Although the absolute numbers of the other γδ T-cell subsets were also affected, the observed decreases were far less pronounced (Fig. 3F).

We hypothesized that macrophages would be required for Ly-6C^{-} CD44^{hi} γδ T-cell retention within SLOs. In such a model, macrophage depletion would lead to the egress of Ly-6C^{-} CD44^{hi} γδ T cells from SLOs and that would account for the significant drop in absolute numbers observed in mice treated 7 days with PLX3397. The membrane receptor S1PR1, by allowing T cells to respond to the sphingolipid S1P present within efferent lymph, is the central mediator of lymphocyte egress from SLOs (31, 32). First, we studied S1PR1 expression by γδ T-cell subsets recovered from pLNs, mLNs and the spleen (Fig. S3). We found that Ly-6C^{-} CD44^{hi} γδ T cells from peripheral and mesenteric LNs exhibited higher

S1PR1 surface levels than the other γδ T-cell subsets. Ly-6C^{-} CD44^{hi} γδ T cells should be thus highly sensitive to S1P gradients. Then, C57BL/6 mice were fed with PLX3397 chow and daily injected or not for 7 days with FTY720 (Fig. 3G). Interestingly, FTY720 injections fully abrogated the strong decrease in Ly-6C^{-} CD44^{hi} γδ T-cell absolute numbers provoked by the PLX3397 treatment in both pLNs and mLNs (Fig. 3H). These results suggest that CSF1R inhibitor administration is not toxic to γδ T cells but rather allow them to egress from LNs through a S1PR1 dependent mechanism. Of note, FTY720 administration did not abolish the effect of the PLX3397 treatment in the spleen but rather accentuated the observed decrease of the absolute number of Ly-6C^{-} CD44^{hi} γδ T-cells (Fig. 3G). That could be explained by the duration of the S1PR1 agonist treatment. More precisely, it has already been described that whereas a single injection of FTY720 induces T-cell sequestration in the spleen (33 , 34), a prolonged FTY720 treatment rather leads, in this SLO, to a decrease in the absolute numbers of T lymphocytes (34, 35, 36).

Taken together, these last results suggest that macrophages play a crucial role in the long-term trapping of Ly-6C^{-} CD44^{hi} γδ T lymphocytes within SLOs.

Membrane blebs reveal the close intimacy between Ly-6C^{-} CD44^{hi} γδ T lymphocytes and macrophages in SLOs

It has recently been shown that an important fraction of IL-17-committed T lymphocytes from pLNs could acquire membrane blebs from subcapsular sinus macrophages, reflecting the intimacy of the crosstalk between these 2 cell types (37). We thus examined the proportion of Ly-6C^{-} CD44^{hi}, Ly-6C^{+} CD44^{hi} and CD44^{lo} γδ T lymphocytes expressing macrophage markers such as CD11b, F4/80 and CD169 (Fig. 4A-B). Expression of these 3 molecules was solely detected on the cell surface of Ly-6C^{-} CD44^{hi} γδ T cells. Interestingly, the surface expression of CD11b, F4/80 and CD169 by Ly-6C^{-} CD44^{hi} γδ T lymphocytes seemed to vary depending

on the location of these cells (pLNs vs mLNs vs the spleen; Fig. 4B) suggesting the ability of Ly-6C$^-$ CD44^{hi} γδ T lymphocytes to initiate intimate crosstalk with various macrophage subsets such as subcapsular sinus macrophages (CD11b$^+$ F4/80$^-$ CD169$^+$), medullary sinus macrophages (CD11b$^+$ F4/80$^+$ CD169$^+$) or spleen red pulp macrophages (CD11b$^-$ F4/80$^+$ CD169$^-$) (38 , 39, 40). More precisely, the observed proportions of Ly-6C$^-$ CD44^{hi} γδ T cells acquiring CD11b, F4/80 and CD169 expression suggest that these cells interact preferentially with subcapsular and medullary sinus macrophages within pLNs (30% of Ly-6C$^-$ CD44^{hi} γδ T cells from pLNs expressed CD11b and CD169 whereas only 15% expressed F4/80), with medullary sinus macrophages in mLNs [equal proportions (15%) of cells from mLNs expressing CD11b, F4/80 and CD169] and with red pulp macrophages in the spleen (Ly-6C$^-$ CD44^{hi} γδ T cells only expressed F4/80) (Fig. 4B and Fig. S4).

Using the PLX3397$^+$ feeding strategy, we then studied the consequences of macrophage depletion on the expression of macrophage markers by Ly-6C$^-$ CD44^{hi} γδ T lymphocytes (Fig. 4C). Following PLX3397 treatment, there was a gradual decrease with time in the proportion of SLO Ly-6C$^-$ CD44^{hi} γδ T cells expressing CD11b, F4/80 or CD169 (Fig. 4D). These latter results confirm that the expression of CD11b, F4/80 and CD169 by this γδ T-cell subset results from the transfer of membrane blebs from macrophages to γδ T cells.

Altogether, our results suggest that Ly-6C$^-$ CD44^{hi} γδ T lymphocytes initiate strong adhesive interactions with macrophages that may lead to their long-term retention within SLOs.

RORγt expression allows to determine the localization of resident γδ T cells within pLNs

We have described above a clear enrichment in IL-17-producing cells among γδ T cells in LNs, 48 hours after blocking T-cell entry into these SLOs (Fig. 1E-F). We thus hypothesized that the expression of the transcription factor RORγt may allow a precise identification of resident γδ T cells in SLOs. We first evaluated the proportion of Ly-6C$^-$ CD44^{hi}, Ly-6C$^+$

317 CD44^{hi} and CD44^{lo} γδ T lymphocytes expressing RORγt in SLOs by using RORγt-GFP
318 transgenic mice (Fig. 5A-B). In agreement with the fact that only Ly-6C^{-} CD44^{hi} γδ T
319 lymphocytes are able to produce IL-17 (15), we found that RORγt expression was restricted to
320 these cells. Surprisingly, the proportion of RORγt^{+} cells within Ly-6C^{-} CD44^{hi} γδ T cells
321 differed considerably depending on the organ studied. Indeed, whereas the vast majority
322 (~80%) of Ly-6C^{-} CD44^{hi} γδ T lymphocytes recovered from pLNs expressed RORγt, this
323 proportion was quite lower in mLNs and the spleen (Fig. 5B). We then examined the
324 expression of RORγt by LN-resident γδ T lymphocytes 48 hours after blocking T-cell entry
325 (Fig. 5C-E). In pLNs, after treatment, the proportion of Ly-6C^{-} CD44^{hi} γδ T cells expressing
326 RORγt was significantly higher than in pLNs from control mice (Fig. 5D). Accordingly, 48
327 hours after blocking T-cell entry, the recovery of RORγt^{+} Ly-6C^{-} CD44^{hi} γδ T cells was far
328 better than the recovery observed for their RORγt^{-} cell counterparts (Fig. 5E). This was not
329 the case for mLNs as in this SLO, RORγt^{-} Ly-6C^{-} CD44^{hi} γδ T cells were more efficiently
330 retained after treatment than RORγt^{+} Ly-6C^{-} CD44^{hi} γδ T cells (Fig. 5D-E).

331 Altogether, these results suggest that the expression of RORγt can be considered as a reliable
332 marker to identify resident γδ T cells within pLNs (but not in mLNs). **T**hus, in order to study
333 the location of resident γδ T cells in pLNs, we imaged pLN slices recovered from RORγt-GFP
334 mice by immunofluorescence microscopy (Fig. 5F-H). In line with the capacity of Ly-6C^{-}
335 CD44^{hi} γδ T lymphocytes to acquire membrane blebs from subcapsular and medullary sinus
336 macrophages, we clearly observed that RORγt^{+} γδ T cells (the majority of which are resident
337 cells within pLNs) were localized close to CD169^{+} sinus macrophages (Fig. 5F-G).
338 Quantification of the distance between RORγt^{-} or RORγt^{+} γδ T cells and CD169^{+} cells
339 confirmed that RORγt^{+} γδ T cells were very significantly far closer to CD169^{+} cells than their
340 RORγt^{-} cell counterparts (Fig. 5H). Such a close vicinity may help explaining the capacity of

Ly-6C^{-} CD44^{hi} γδ T cells to acquire macrophage-related surface markers and such interactions may lead to the long-term retention of these cells within SLOs.

Ly-6C^{-} CD44^{hi} γδ T lymphocytes from SLOs respond rapidly *in vivo* to LPS challenge

As described above, our results suggest that Ly-6C^{-} CD44^{hi} γδ T lymphocytes initiate strong adhesive interactions with macrophages that may lead to their long-term retention within SLOs. In addition, we observed that resident RORγt^{+} γδ T cells were localized close to CD169^{+} sinus macrophages within pLNs. We thus hypothesized that SLO resident γδ T cells could represent sentinels surveying the pathogen-exposed surface of SLOs.

To address this issue, RORγt-GFP transgenic mice were injected i.v. with LPS. IL-17 and IFNγ productions by Ly-6C^{-} CD44^{hi} γδ T cells recovered from pLNs, mLNs and the spleen were then analyzed 3 hours later (Fig. 5I). We observed that, in all SLOs, around 20% of Ly-6C^{-} CD44^{hi} γδ T cells were already producing IL-17 in response to LPS challenge at this early time-point (Fig. 5J). In addition, we noticed that IL-17 production was restricted to RORγt expressing cells (Fig. 5K). Of note, in the same setting, we detected a small proportion of IFNγ-producing Ly-6C^{-} CD44^{hi} γδ T cells in the spleen and this IFNγ production was restricted to RORγt^{-} cells (Fig. 5J-K). The capacity of Ly-6C^{-} CD44^{hi} γδ T cells to rapidly produce IL-17 upon LPS challenge strongly suggest that these SLO resident γδ T cells could play a crucial surveying role to protect these organs from infections.

DISCUSSION

To achieve their surveying task for foreign antigens and survival signals, peripheral T cells have been described as having a nomadic existence between blood, SLOs and lymph in the steady state (16 , 17). Transit times within SLOs should be (a) not too long as T cells must continuously scan antigen-presenting cells (APCs) from different LNs in order to find where the next pathogen will cross the epithelial barrier, but also (b) not too rapid to avoid missing the rare APCs presenting their specific antigen in SLOs in the early phases of an infection. However, in parallel to that model, recent findings highlight the existence of T cells residing for long periods of time within non-lymphoid tissues (41). More precisely, subsets of $CD8^+$ and $CD4^+$ αβ T cells but also subsets of NK cells, NKT cells and γδ T cells have been shown to reside within non-lymphoid tissues such as the skin, gut, lungs or adipose tissue providing a rapid and efficient protection against reinfection by tissue-tropic pathogens but also promoting the repair of damaged tissues (42 , 43 , 44 , 45 , 46 , 47).

In the present paper, using injection of integrin-neutralizing antibodies and parabiosis strategies, we highlight the existence of γδ T cells residing in the steady state in the SLOs of specific pathogen-free mice. In line with our results, Zhang et al. have recently shown that innate-like T cells defined as expressing high surface levels of CD127 and CCR6, among which about one fourth corresponds to γδ T cells, accumulated near the subcapsular sinus in pLNs (32). Here, we confirm and extend these observations. First, while Zhang et al. examined the amount of cell exchange 2 weeks after surgery in parabiotic mice or 2 days after T-cell photoconversion in photoconvertible fluorescence protein Kaede transgenic mice, our parabiosis experiments clearly showed that full chimerism between the 2 parabionts was still not reached in pLNs for Ly-$6C^-$ $CD44^{hi}$ γδ T cells at least up to 2 months after surgery (Fig. 2). Thus, we here demonstrate the long-term residency of these cells within pLNs. Second, we showed that the long-term retention of Ly-$6C^-$ $CD44^{hi}$ γδ T cells was not a peculiar feature of

pLNs as it also applies to mLNs and the spleen. Third, while we confirmed that in pLNs, innate-like Ly-6C^{-} CD44^{hi} γδ T lymphocytes were located close to subcapsular sinus macrophages and were able to acquire, from this vicinity, the apparent expression of CD11b and CD169, our results strongly suggest that other subsets of macrophages are involved in the retention of these cells within SLOs (see below). Finally, we have also studied the behavior of the other γδ T-cell subsets (i.e. Ly-6C^{+} CD44^{hi} and Ly-6C$^{-/+}$ CD44^{low} γδ T cells) in SLOs and showed that whatever their naïve-like or memory-like phenotype, they corresponded to circulating cells.

In addition to the CD11b and CD169 markers, about half of CD11b-expressing innate-like γδ T cells in pLNs and all of them in mLNs were also acquiring F4/80 expression (Fig. 4B). Like for CD11b and CD169, F4/80 surface expression by γδ T cells decreased gradually following *in vivo* macrophage depletion suggesting that innate-like γδ T cells are not only interacting with subcapsular (CD11b^{+} F4/80^{-} CD169^{+}) sinus macrophages but also with medullary sinus (CD11b^{+} F4/80^{+} CD169^{+}) macrophages. Finally, our parabiosis experiments show that a fraction of Ly-6C^{-} CD44^{hi} γδ T cells are also residing for long periods of time in the spleen. In this SLO, only F4/80 was detected at the cell surface of Ly-6C^{-} CD44^{hi} γδ T cells. This latter result suggests that resident γδ T lymphocytes are interacting with splenic red pulp (CD11b^{-} F4/80^{+} CD169^{-}) macrophages. Such a hypothesis would be in agreement with previous studies that have observed a preferential localization of human and mice γδ T lymphocytes within the red pulp of the spleen (48 , 49). Interactions between tissue resident γδ T cells and F4/80^{+} macrophages have been reported in the lungs in mice (50). Indeed, it has been shown that pulmonary resident γδ T cells had an intrinsic preference to interact with F4/80^{+} macrophages (51). These continuous interactions would be important for their protective role as sentinels of airways and lung tissues.

Altogether, our data suggest that the precise "nature" of resident γδ T cells but also of the macrophages involved in their retention varies according to the secondary lymphoid organs analyzed (pLNs vs mLNs vs the spleen). Indeed, whereas in pLNs, the residence of Ly-6C$^-$ CD44^{hi} γδ T cells was mostly restricted to RORγt$^+$ cells, RORγt$^-$ cells were more efficiently trapped in mLNs than their RORγt$^+$ cell counterparts. Furthermore, whereas both subcapsular and medullary sinus macrophages would be involved in the retention of Ly-6C$^-$ CD44^{hi} γδ T cells in pLNs, the role of subcapsular sinus macrophages would be less crucial in mLNs and the spleen. Indeed, medullary sinus and red pulp macrophages appear as the main actors implied in the retention of γδ T cells in mLNs and the spleen respectively. Sinus and red pulp macrophages have a propensity to capture particulate material arriving in the lymph and the blood (52-54). Thus, we hypothesize that resident Ly-6C$^-$ CD44^{hi} γδ T cells could play a critical surveillance role in protecting SLOs from infections. In our previous study, we have showed that Ly-6C$^-$ CD44^{hi} γδ T cells were possessing innate-like properties such as the ability to respond directly to TLR ligands *in vitro* (15). Here, we have found that Ly-6C$^-$ CD44^{hi} γδ T cells from SLOs were rapidly able to produce IL-17 *in vivo* in response to LPS challenge. In this setting, LPS may activate them directly or indirectly through the induction of IL-23 and IL-1beta production by neighboring macrophages as it has been described that RORγt$^+$ γδ T cells express IL-23R and produce IL-17 in response to IL-1beta and IL-23, without T-cell receptor engagement (6). We are thus proposing that resident γδ T cells and macrophages could have complementary roles and may represent a major barrier blocking the systemic spread of pathogens within SLOs by providing rapid innate responses.

ACKNOWLEDGMENTS

We are grateful to Plexxikon Inc. for providing the PLX3397 inhibitor. We thank the Cochin Cytometry and Immunobiology (CIBIO), Cochin imaging photonic (IMAG'IC) and Cochin Animal Core facilities.

FOOTNOTES

This work was supported by grants from la Ligue contre le cancer, the Association pour la Recherche contre le Cancer, and the Fondation pour la Recherche Médicale. M.R. was supported by a fellowship from Fondation pour la Recherche Médical. A. A. V. and P. H. were supported by a PhD fellowship from the "Ligue contre le Cancer" and from INSERM. V. G. was supported by a PhD fellowship from the French Ministry of National Education, Research, and Technology. E.P. was supported by a fellowship from Fondation de France.

REFERENCES

1. Chien, Y. H., C. Meyer, and M. Bonneville. 2014. gammadelta T cells: first line of defense and beyond. *Annu Rev Immunol* 32: 121-155.

2. Nanno, M., Y. Kanari, T. Naito, N. Inoue, T. Hisamatsu, H. Chinen, K. Sugimoto, Y. Shimomura, H. Yamagishi, T. Shiohara, S. Ueha, K. Matsushima, M. Suematsu, A. Mizoguchi, T. Hibi, A. K. Bhan, and H. Ishikawa. 2008. Exacerbating role of gammadelta T cells in chronic colitis of T-cell receptor alpha mutant mice. *Gastroenterology* 134: 481-490.

3. Mombaerts, P., E. Mizoguchi, M. J. Grusby, L. H. Glimcher, A. K. Bhan, and S. Tonegawa. 1993. Spontaneous development of inflammatory bowel disease in T cell receptor mutant mice. *Cell* 75: 274-282.

4. Roark, C. L., J. D. French, M. A. Taylor, A. M. Bendele, W. K. Born, and R. L. O'Brien. 2007. Exacerbation of collagen-induced arthritis by oligoclonal, IL-17-producing gamma delta T cells. *J Immunol* 179: 5576-5583.

5. Keystone, E. C., C. Rittershaus, N. Wood, K. M. Snow, J. Flatow, J. C. Purvis, L. Poplonski, and P. C. Kung. 1991. Elevation of a gamma delta T cell subset in peripheral blood and synovial fluid of patients with rheumatoid arthritis. *Clin Exp Immunol* 84: 78-82.

6. Sutton, C. E., S. J. Lalor, C. M. Sweeney, C. F. Brereton, E. C. Lavelle, and K. H. Mills. 2009. Interleukin-1 and IL-23 induce innate IL-17 production from gammadelta T cells, amplifying Th17 responses and autoimmunity. *Immunity* 31: 331-341.

7. Wucherpfennig, K. W., P. Hollsberg, J. H. Richardson, D. Benjamin, and D. A. Hafler. 1992. T-cell activation by autologous human T-cell leukemia virus type I-infected T-cell clones. *Proc Natl Acad Sci U S A* 89: 2110-2114.

8. Street, S. E., Y. Hayakawa, Y. Zhan, A. M. Lew, D. MacGregor, A. M. Jamieson, A. Diefenbach, H. Yagita, D. I. Godfrey, and M. J. Smyth. 2004. Innate immune surveillance of spontaneous B cell lymphomas by natural killer cells and gammadelta T cells. *J Exp Med* 199: 879-884.

9. Girardi, M., D. E. Oppenheim, C. R. Steele, J. M. Lewis, E. Glusac, R. Filler, P. Hobby, B. Sutton, R. E. Tigelaar, and A. C. Hayday. 2001. Regulation of cutaneous malignancy by gammadelta T cells. *Science* 294: 605-609.

10. Liu, Z., I. E. Eltoum, B. Guo, B. H. Beck, G. A. Cloud, and R. D. Lopez. 2008. Protective immunosurveillance and therapeutic antitumor activity of gammadelta T cells demonstrated in a mouse model of prostate cancer. *J Immunol* 180: 6044-6053.

11. Gao, Y., W. Yang, M. Pan, E. Scully, M. Girardi, L. H. Augenlicht, J. Craft, and Z. Yin. 2003. Gamma delta T cells provide an early source of interferon gamma in tumor immunity. *J Exp Med* 198: 433-442.

12. Lanca, T., M. F. Costa, N. Goncalves-Sousa, M. Rei, A. R. Grosso, C. Penido, and B. Silva-Santos. 2013. Protective role of the inflammatory CCR2/CCL2 chemokine pathway through recruitment of type 1 cytotoxic gammadelta T lymphocytes to tumor beds. *J Immunol* 190: 6673-6680.

13. Lafont, V., F. Sanchez, E. Laprevotte, H. A. Michaud, L. Gros, J. F. Eliaou, and N. Bonnefoy. 2014. Plasticity of gammadelta T Cells: Impact on the Anti-Tumor Response. *Front Immunol* 5: 622.

14. Coffelt, S. B., K. Kersten, C. W. Doornebal, J. Weiden, K. Vrijland, C. S. Hau, N. J. Verstegen, M. Ciampricotti, L. J. Hawinkels, J. Jonkers, and K. E. de Visser. 2015. IL-17-producing gammadelta T cells and neutrophils conspire to promote breast cancer metastasis. *Nature* 522: 345-348.

15. Lombes, A., A. Durand, C. Charvet, M. Riviere, N. Bonilla, C. Auffray, B. Lucas, and B. Martin. 2015. Adaptive Immune-like gamma/delta T Lymphocytes Share Many Common Features with Their alpha/beta T Cell Counterparts. *J Immunol* 195: 1449-1458.

16. von Andrian, U. H., and T. R. Mempel. 2003. Homing and cellular traffic in lymph nodes. *Nat Rev Immunol* 3: 867-878.

17. Gowans, J. L., and E. J. Knight. 1964. The Route of Re-Circulation of Lymphocytes in the Rat. *Proc R Soc Lond B Biol Sci* 159: 257-282.

18. Mandl, J. N., R. Liou, F. Klauschen, N. Vrisekoop, J. P. Monteiro, A. J. Yates, A. Y. Huang, and R. N. Germain. 2012. Quantification of lymph node transit times reveals differences in antigen surveillance strategies of naive CD4+ and CD8+ T cells. *Proc Natl Acad Sci U S A* 109: 18036-18041.

19. Vantourout, P., and A. Hayday. 2013. Six-of-the-best: unique contributions of gammadelta T cells to immunology. *Nat Rev Immunol* 13: 88-100.

20. Silva-Santos, B., K. Serre, and H. Norell. 2015. gammadelta T cells in cancer. *Nat Rev Immunol* 15: 683-691.

21. Akitsu, A., H. Ishigame, S. Kakuta, S. H. Chung, S. Ikeda, K. Shimizu, S. Kubo, Y. Liu, M. Umemura, G. Matsuzaki, Y. Yoshikai, S. Saijo, and Y. Iwakura. 2015. IL-1 receptor antagonist-deficient mice develop autoimmune arthritis due to intrinsic activation of IL-17-producing CCR2(+)Vgamma6(+)gammadelta T cells. *Nat Commun* 6: 7464.

22. Ramirez-Valle, F., E. E. Gray, and J. G. Cyster. 2015. Inflammation induces dermal Vgamma4+ gammadeltaT17 memory-like cells that travel to distant skin and accelerate secondary IL-17-driven responses. *Proc Natl Acad Sci U S A* 112: 8046-8051.

23. Penido, C., M. F. Costa, M. C. Souza, K. A. Costa, A. L. Candea, C. F. Benjamim, and M. Henriques. 2008. Involvement of CC chemokines in gammadelta T lymphocyte trafficking during allergic inflammation: the role of CCL2/CCR2 pathway. *Int Immunol* 20: 129-139.

24. Hochweller, K., J. Striegler, G. J. Hammerling, and N. Garbi. 2008. A novel CD11c.DTR transgenic mouse for depletion of dendritic cells reveals their requirement for homeostatic proliferation of natural killer cells. *Eur J Immunol* 38: 2776-2783.

25. Lochner, M., L. Peduto, M. Cherrier, S. Sawa, F. Langa, R. Varona, D. Riethmacher, M. Si-Tahar, J. P. Di Santo, and G. Eberl. 2008. In vivo equilibrium of proinflammatory IL-17+ and regulatory IL-10+ Foxp3+ RORgamma t+ T cells. *J Exp Med* 205: 1381-1393.

26. Le Campion, A., A. Pommier, A. Delpoux, L. Stouvenel, C. Auffray, B. Martin, and B. Lucas. 2012. IL-2 and IL-7 determine the homeostatic balance between the regulatory and conventional CD4+ T cell compartments during peripheral T cell reconstitution. *J Immunol* 189: 3339-3346.

27. Pommier, A., A. Audemard, A. Durand, R. Lengagne, A. Delpoux, B. Martin, L. Douguet, A. Le Campion, M. Kato, M. F. Avril, C. Auffray, B. Lucas, and A. Prevost-Blondel. 2013. Inflammatory monocytes are potent antitumor effectors controlled by regulatory CD4+ T cells. *Proc Natl Acad Sci U S A* 110: 13085-13090.

28. Delpoux, A., P. Yakonowsky, A. Durand, C. Charvet, M. Valente, A. Pommier, N. Bonilla, B. Martin, C. Auffray, and B. Lucas. 2014. TCR signaling events are required for maintaining CD4 regulatory T cell numbers and suppressive capacities in the periphery. *J Immunol* 193: 5914-5923.

29. Martin, B., C. Auffray, A. Delpoux, A. Pommier, A. Durand, C. Charvet, P. Yakonowsky, H. de Boysson, N. Bonilla, A. Audemard, T. Sparwasser, B. L. Salomon, B. Malissen, and B. Lucas. 2013. Highly self-reactive naive CD4 T cells are prone to differentiate into regulatory T cells. *Nat Commun* 4: 2209.

30. Narayan, K., K. E. Sylvia, N. Malhotra, C. C. Yin, G. Martens, T. Vallerskog, H. Kornfeld, N. Xiong, N. R. Cohen, M. B. Brenner, L. J. Berg, J. Kang, and C. Immunological Genome Project. 2012. Intrathymic programming of effector fates in three molecularly distinct gammadelta T cell subtypes. *Nat Immunol* 13: 511-518.

31. Cyster, J. G., and S. R. Schwab. 2012. Sphingosine-1-phosphate and lymphocyte egress from lymphoid organs. *Annu Rev Immunol* 30: 69-94.

32. Zhang, Y., T. L. Roth, E. E. Gray, H. Chen, L. B. Rodda, Y. Liang, P. Ventura, S. Villeda, P. R. Crocker, and J. G. Cyster. 2016. Migratory and adhesive cues controlling innate-like lymphocyte surveillance of the pathogen-exposed surface of the lymph node. *Elife* 5.

33. Mandala, S., R. Hajdu, J. Bergstrom, E. Quackenbush, J. Xie, J. Milligan, R. Thornton, G. J. Shei, D. Card, C. Keohane, M. Rosenbach, J. Hale, C. L. Lynch, K. Rupprecht, W. Parsons, and H. Rosen. 2002. Alteration of lymphocyte trafficking by sphingosine-1-phosphate receptor agonists. *Science* 296: 346-349.

34. Morris, M. A., D. R. Gibb, F. Picard, V. Brinkmann, M. Straume, and K. Ley. 2005. Transient T cell accumulation in lymph nodes and sustained lymphopenia in mice treated with FTY720. *Eur J Immunol* 35: 3570-3580.

35. Hofmann, M., V. Brinkmann, and H. G. Zerwes. 2006. FTY720 preferentially depletes naive T cells from peripheral and lymphoid organs. *Int Immunopharmacol* 6: 1902-1910.

36. Schwab, S. R., and J. G. Cyster. 2007. Finding a way out: lymphocyte egress from lymphoid organs. *Nat Immunol* 8: 1295-1301.

37. Gray, E. E., S. Friend, K. Suzuki, T. G. Phan, and J. G. Cyster. 2012. Subcapsular sinus macrophage fragmentation and CD169+ bleb acquisition by closely associated IL-17-committed innate-like lymphocytes. *PLoS One* 7: e38258.

38. Gray, E. E., and J. G. Cyster. 2012. Lymph node macrophages. *J Innate Immun* 4: 424-436.

39. Franken, L., M. Schiwon, and C. Kurts. 2016. Macrophages: sentinels and regulators of the immune system. *Cell Microbiol* 18: 475-487.

40. Franken, L., M. Klein, M. Spasova, A. Elsukova, U. Wiedwald, M. Welz, P. Knolle, M. Farle, A. Limmer, and C. Kurts. 2015. Splenic red pulp macrophages are intrinsically superparamagnetic and contaminate magnetic cell isolates. *Sci Rep* 5: 12940.

41. Mueller, S. N., and L. K. Mackay. 2016. Tissue-resident memory T cells: local specialists in immune defence. *Nat Rev Immunol* 16: 79-89.

42. Turner, D. L., and D. L. Farber. 2014. Mucosal resident memory CD4 T cells in protection and immunopathology. *Front Immunol* 5: 331.

43. Panduro, M., C. Benoist, and D. Mathis. 2016. Tissue Tregs. *Annu Rev Immunol* 34: 609-633.

44. Peng, H., X. Jiang, Y. Chen, D. K. Sojka, H. Wei, X. Gao, R. Sun, W. M. Yokoyama, and Z. Tian. 2013. Liver-resident NK cells confer adaptive immunity in skin-contact inflammation. *J Clin Invest* 123: 1444-1456.

45. Lynch, L., X. Michelet, S. Zhang, P. J. Brennan, A. Moseman, C. Lester, G. Besra, E. E. Vomhof-Dekrey, M. Tighe, H. F. Koay, D. I. Godfrey, E. A. Leadbetter, D. B. Sant'Angelo, U. von Andrian, and M. B. Brenner. 2015. Regulatory iNKT cells lack expression of the transcription factor PLZF and control the homeostasis of T(reg) cells and macrophages in adipose tissue. *Nat Immunol* 16: 85-95.

46. Di Marco Barros, R., N. A. Roberts, R. J. Dart, P. Vantourout, A. Jandke, O. Nussbaumer, L. Deban, S. Cipolat, R. Hart, M. L. Iannitto, A. Laing, B. Spencer-Dene, P. East, D. Gibbons, P. M. Irving, P. Pereira, U. Steinhoff, and A. Hayday. 2016. Epithelia Use Butyrophilin-like Molecules to Shape Organ-Specific gammadelta T Cell Compartments. *Cell* 167: 203-218 e217.

47. O'Brien, R. L., and W. K. Born. 2015. Dermal gammadelta T cells--What have we learned? *Cell Immunol* 296: 62-69.

48. Bordessoule, D., P. Gaulard, and D. Y. Mason. 1990. Preferential localisation of human lymphocytes bearing gamma delta T cell receptors to the red pulp of the spleen. *J Clin Pathol* 43: 461-464.

49. Nolte, M. A., E. N. Hoen, A. van Stijn, G. Kraal, and R. E. Mebius. 2000. Isolation of the intact white pulp. Quantitative and qualitative analysis of the cellular composition of the splenic compartments. *Eur J Immunol* 30: 626-634.

50. Nanno, M., T. Shiohara, H. Yamamoto, K. Kawakami, and H. Ishikawa. 2007. gammadelta T cells: firefighters or fire boosters in the front lines of inflammatory responses. *Immunol Rev* 215: 103-113.

51. Wands, J. M., C. L. Roark, M. K. Aydintug, N. Jin, Y. S. Hahn, L. Cook, X. Yin, J. Dal Porto, M. Lahn, D. M. Hyde, E. W. Gelfand, R. J. Mason, R. L. O'Brien, and W. K. Born. 2005. Distribution and leukocyte contacts of gammadelta T cells in the lung. *J Leukoc Biol* 78: 1086-1096.

52. Carrasco, Y. R., and F. D. Batista. 2007. B cells acquire particulate antigen in a macrophage-rich area at the boundary between the follicle and the subcapsular sinus of the lymph node. *Immunity* 27: 160-171.

53. Cinamon, G., M. A. Zachariah, O. M. Lam, F. W. Foss, Jr., and J. G. Cyster. 2008. Follicular shuttling of marginal zone B cells facilitates antigen transport. *Nat Immunol* 9: 54-62.

54. Junt, T., E. A. Moseman, M. Iannacone, S. Massberg, P. A. Lang, M. Boes, K. Fink, S. E. Henrickson, D. M. Shayakhmetov, N. C. Di Paolo, N. van Rooijen, T. R. Mempel, S. P. Whelan, and U. H. von

590 Andrian. 2007. Subcapsular sinus macrophages in lymph nodes clear lymph-borne viruses and present
591 them to antiviral B cells. *Nature* 450: 110-114.

592

FIGURE LEGENDS

Figure 1: An important proportion of Ly-6C$^-$ CD44^{hi} γδ T lymphocytes is trapped in LNs in the steady state

C57BL/6 mice have been injected i.p. with integrin-neutralizing anti-LFA-1 (αL) and anti-VLA-4 (α4) antibodies. Two days after treatment, pLNs, mLNs and spleen (Spl.) were recovered separately. (A) Diagram illustrating the experimental model. (B) CD44/Ly-6C dot-plots for gated TCRγδ$^+$ cells recovered from pLNs of representative control and treated mice. Numbers on FACS dot-plots indicate the percentage of Ly-6C$^-$ CD44^{hi} γδ T cells among the γδ T lymphocyte compartment (C) Pie charts illustrating the proportions of γδ T-cell subsets recovered from pLNs, mLNs and spleen (Spl.) of control (Ctrl.) and treated mice. (D) Percentage of γδ T cell-subset recovery within pLNs, mLNs and spleen (Spl.) of anti-αL and anti-α4 treated mice. The percentage of recovery was calculated by dividing the absolute numbers in treated mice by the mean absolute number obtained in untreated animals. (E) Percentage of Vγ1.1$^+$ and Vγ2$^+$ cells among Ly-6C$^-$ CD44^{hi} γδ T cells recovered from pLNs and mLNs of control (Ctrl.) and anti-αL and anti-α4 treated mice. (F) IL-17/IFNγ dot-plots for gated TCRγδ$^+$ cells recovered from pLNs of representative control and treated mice. (G) Proportion of IL-17- and IFNγ-producing TCRγδ$^+$ cells recovered from peripheral and mesenteric LNs of control and treated mice. (H-I) C57BL/6 mice have been injected i.p. every 2 days during 6 days with 200μg of both integrin-neutralizing Abs and analyzed 24 hours later. (H) Diagram illustrating the experimental model. (I) Percentage of γδ T-cell subset recovery within pLNs, mLNs and spleen (Spl.) of 6 days treated mice.

(C, D, E, G, I) Results are shown as means±s.e.m. for at least two mice per group per experiment, from at least three independent experiments and each point indicates an individual mouse. Significance of differences between two series of results was assessed

using a two-tailed paired (D, H) or unpaired (C, F) Student's t-test. Values of $P<0.05$ were considered as statistically significant (*$P<0.05$; **$P<0.01$; ***$P<0.001$; and **** $P<0.0001$).

Figure 2: Ly-6C^{-} CD44^{hi} γδ T lymphocytes are largely long-term SLO-resident cells in the steady state

Parabiotic mice were established between CD45.1 and CD45.2 C57BL/6 mice. Four weeks after surgery, parabiotic pairs were analyzed. (A) Diagram illustrating the experimental model. (B) Proportions of host cells, CD45.1^{+} for the CD45.1 parabiont and CD45.2^{+} for the CD45.2 parabiont, among the indicated γδ T-cell subsets recovered from pLNs, mLNs and spleen (Spl.) from parabiotic pairs. (C) IL-17 and IFNγ dot-plots for gated TCRγδ^{+} cells recovered from spleen of representative parabiotic mice and percentage of host cells among these IL-17- and IFNγ-producing γδ T cells. (D-E) Parabiotic mice were established between CD45.1 and CD45.2 C57BL/6 mice and analyzed 8 weeks after surgery. (D) Diagram illustrating the experimental model. (E) Proportions of host cells among the indicated γδ T-cell subsets recovered from pLNs, mLNs and spleen (Spl.) from parabiotic pairs. Results are shown as means±s.e.m. for at least three mice per group per experiment, from at least three independent experiments.

Figure 3: Macrophages are responsible for the long-term trapping of Ly-6C^{-} CD44^{hi} γδ T lymphocytes within SLOs in the steady state

(A-B) C57BL/6 and C57BL/6 μMT mice have been treated or not with integrin-neutralizing antibodies and analyzed 48 hours later. (A) Diagram illustrating the experimental model. (B) Percentage of γδ T cell-subset recovery (calculated as in figure 1D) within pLNs and mLNs of anti-αL and anti-α4 treated C57BL/6 and C57BL/6 μMT mice. (C-D) C57BL/6 CD11c.DTR

641 mice (designated CD11c.DOG) have been injected or not with integrin-neutralizing
642 antibodies and Diphtheria Toxin (DT). (C) Diagram illustrating the experimental model. (D)
643 Percentage of γδ T cell-subset recovery within pLNs and mLNs of anti-αL and anti-α4 treated
644 control (Ctrl.) and DT injected mice. (E-F) C57BL/6 mice were fed with mouse chow
645 containing or not an inhibitor of CSF1R (PLX3397). Seven days after PLX3397 feeding,
646 pLNs, mLNs and spleen were recovered separately. (E) Diagram illustrating the experimental
647 model. (F) Percentage of γδ T-cell subset recovery within pLNs, mLNs and spleen (Spl.) of
648 PLX3397 fed mice. (G-H) C57BL/6 mice were fed with mouse chow containing or not
649 PLX3397 and daily injected or not with FTY720. Seven days after PLX3397 and FTY
650 treatments, pLNs, mLNs and spleen were recovered separately. (G) Diagram illustrating the
651 experimental model. (H) Absolute numbers of Ly-6C$^-$ CD44^{hi} γδ T cells recovered from
652 pLNs, mLNs and spleen of control (Ctrl.), PLX3397 and PLX3397+FTY720 treated mice. (B,
653 D, F, H) Results are shown as means±s.e.m. for at least three mice per group per experiment,
654 from at least two independent experiments.
655

656 **Figure 4: Membrane blebs reveal the close intimacy between Ly-6C$^-$ CD44^{hi} γδ T**
657 **lymphocytes and macrophage subsets in SLOs**

658 (A) CD11b, F4/80 and CD169 fluorescence histograms of γδ T-cell subsets recovered from
659 pLNs are shown for a representative C57BL/6 mouse. Numbers in each histogram represent
660 the percentage of CD11b$^+$, F4/80$^+$ or CD169$^+$ cells among γδ T-cell subsets. (B) The
661 proportions of CD11b$^+$, F4/80$^+$ or CD169$^+$ cells among γδ T-cell subsets recovered from
662 pLNs, mLNs and spleen (Spl.) of C57BL/6 mice were calculated. (C-D) C57BL/6 mice were
663 fed with mouse chow containing or not an inhibitor of CSF1R (PLX3397). Two, four and
664 seven days after PLX3397 feeding, pLNs, mLNs and spleen were recovered separately. (C)
665 Diagram illustrating the experimental model. (D) The proportions of CD11b$^+$, F4/80$^+$ or

CD169^{+} cells among Ly-6C^{-} CD44^{hi} γδ T cells recovered from pLNs, mLNs and spleen (Spl.) of C57BL/6 mice were calculated. Results are shown as means±s.e.m. for at least three mice per group per experiment, from at least three independent experiments.

Figure 5: RORγt expression allows to determine the location of resident γδ T cells within pLNs

(A) RORγt/TCRγδ dot-plots for gated γδ T-cell subsets recovered from pLNs of a representative C57BL/6 RORγt-GFP mouse. (B) The proportions of RORγt^{+} cells among γδ T-cell subsets recovered from pLNs, mLNs and spleen (Spl.) of C57BL/6 RORγt-GFP mice were calculated. (C-E) C57BL/6 RORγt-GFP mice have been injected i.p. with integrin-neutralizing anti-LFA-1 (αL) and anti-VLA-4 (α4) antibodies. Two days after treatment, pLNs and mLNs were recovered separately. (C) Diagram illustrating the experimental model. (D) The proportions of RORγt^{+} cells among Ly-6C^{-} CD44^{hi} γδ T cells recovered from pLNs and mLNs of treated or untreated mice were calculated. (E) Percentage of RORγt^{+} and RORγt^{-} Ly-6C^{-} CD44^{hi} γδ T-cell recovery (calculated as in figure 1) within pLNs and mLNs of anti-αL and anti-α4 treated mice. Results are shown as means±s.e.m. for at least three mice per group per experiment, from at least three independent experiments.

(F-H) Location of RORγt^{-} and RORγt^{+} γδ T cells within pLNs from C57BL/6 RORγt-GFP mouse has been examined. (F) Representative immunofluorescence TCRγδ, CD169 and RORγt-GFP staining of fixed pLNs slices (maxillary LN is shown here). RORγt^{+} γδ T cells appear in yellow. Squares indicate zoomed areas presented on the figure. (G) Location modeling of RORγt^{-} and RORγt^{+} γδ T lymphocytes within pLNs (maxillary LN is shown here). Coordinates of all RORγt^{-} and RORγt^{+} γδ T cells were calculated from immunofluorescence staining shown in (F) and were then re-applied on CD169 stained LN

690 slice. (H) Distance between RORγt^{-} and RORγt^{+} γδ T lymphocytes and CD169^{+} cells were
691 calculated. (I, J, K) C57BL/6 RORγt-GFP mice were injected i.v. with LPS. Three hours later,
692 cells recovered from pLNs, mLNs and spleen were incubated during 2 hours with Brefeldin A
693 for determination of intracellular cytokine production. (I) Diagram illustrating the
694 experimental model. (J) Percentage of IL-17- and IFNγ-producing cells among Ly-6C^{-} CD44^{hi}
695 γδ T cells recovered from pLNs, mLNs and spleen of control (Ctrl.) and LPS treated mice.
696 (K) Percentage of IL-17- and IFNγ-producing cells among RORγt^{-} and RORγt^{+} Ly-6C^{-} CD44^{hi}
697 γδ T cells recovered from pLNs, mLNs and spleen of LPS treated mice. Results are shown as
698 means±s.e.m. for at least three different LNs slices from three different mice.
699
700
701
702

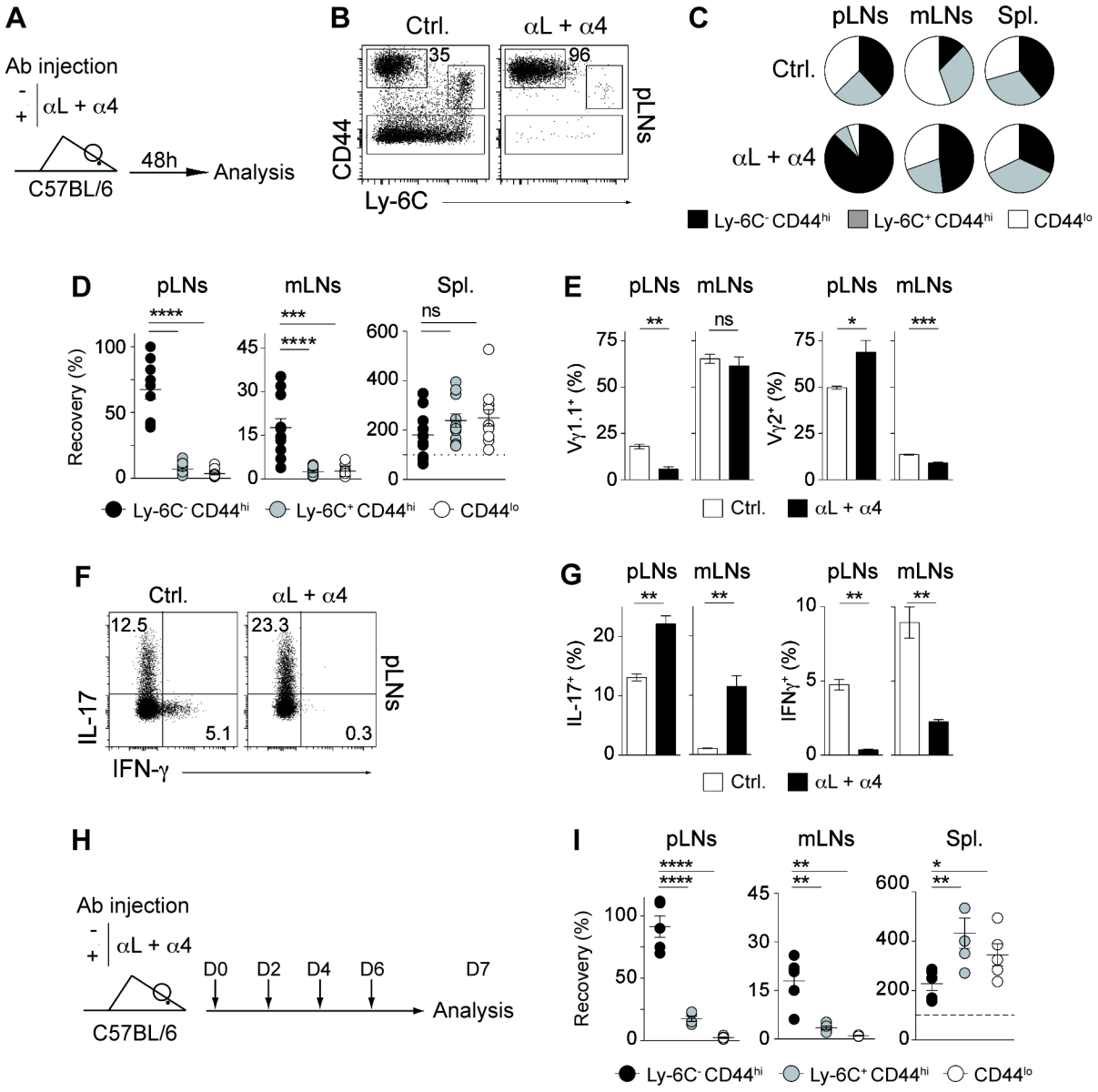
A
Ab injection
αL + α4
C57BL/6
48h
Analysis
B
Ctrl.
αL + α4
35
96
CD44
Ly-6C
pLNs
C
pLNs
mLNs
Spl.
Ctrl.
αL + α4
Ly-6C⁻ CD44hi
Ly-6C⁺ CD44hi
CD44lo
D
pLNs
mLNs
Spl.
Recovery (%)
Ly-6C⁻ CD44hi
Ly-6C⁺ CD44hi
CD44lo
E
pLNs
mLNs
Vγ1.1⁺ (%)
Vγ2⁺ (%)
Ctrl.
αL + α4
F
Ctrl.
αL + α4
12.5
5.1
23.3
0.3
IL-17
IFN-γ
pLNs
G
pLNs
mLNs
IL-17⁺ (%)
IFNγ⁺ (%)
Ctrl.
αL + α4
H
Ab injection
αL + α4
C57BL/6
D0
D2
D4
D6
D7
Analysis
I
pLNs
mLNs
Spl.
Recovery (%)
Ly-6C⁻ CD44hi
Ly-6C⁺ CD44hi
CD44lo

Figure 1

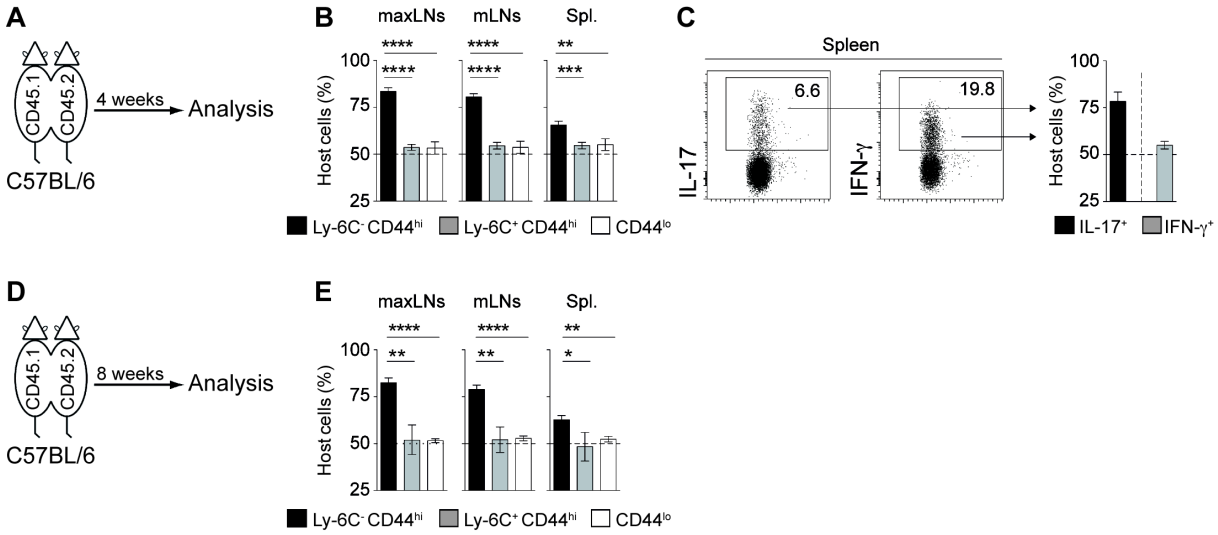

706
707
708

Figure 2

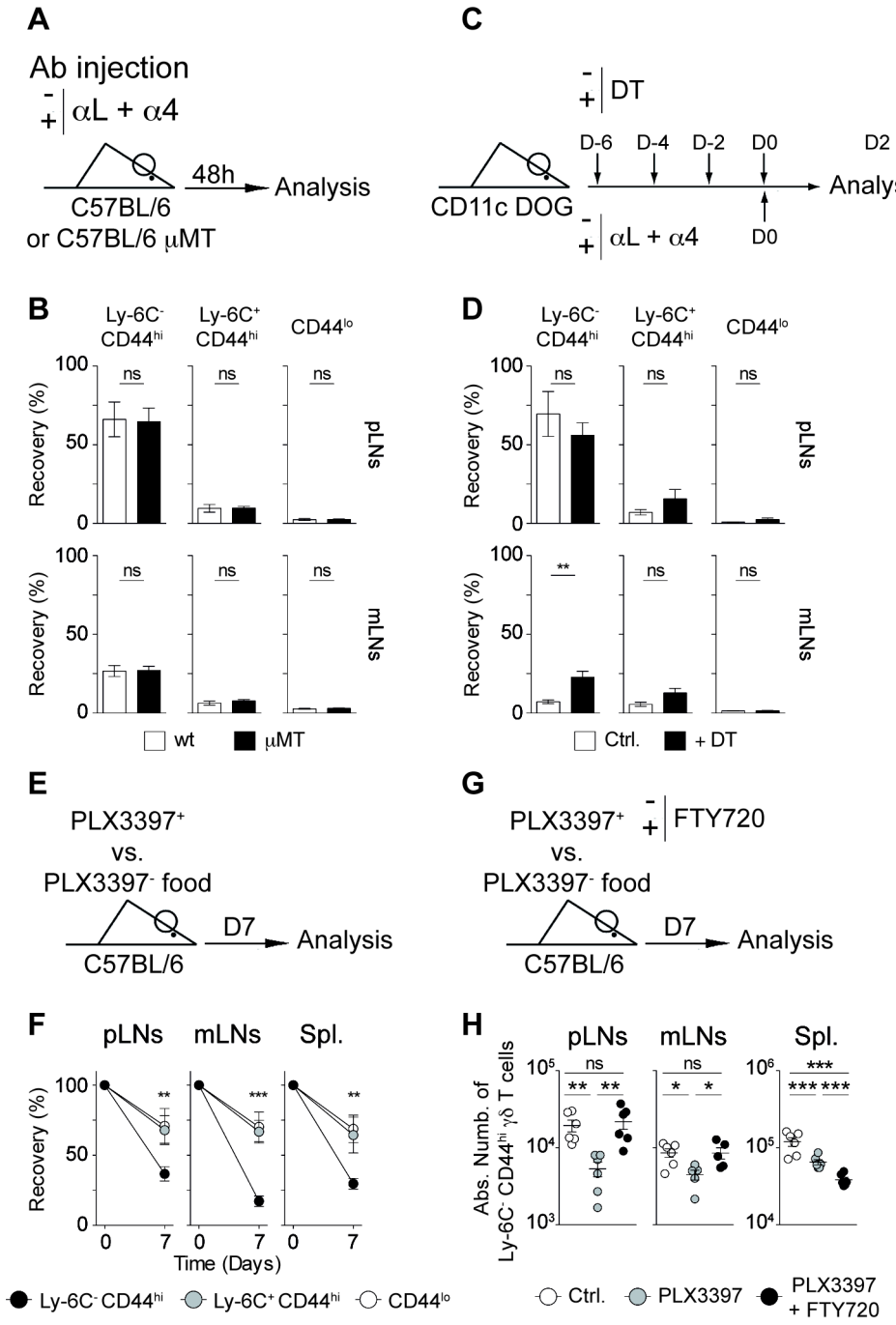
A
Ab injection
- / + αL + α4
48h
Analysis
C57BL/6
or C57BL/6 μMT
C
- / + DT
D-6 D-4 D-2 D0 D2
CD11c DOG
Analysis
- / + αL + α4
D0
B
Ly-6C- CD44hi
Ly-6C+ CD44hi
CD44lo
Recovery (%)
ns
**
pLNs
mLNs
wt
μMT
D
Ctrl.
+ DT
E
PLX3397+ vs. PLX3397- food
D7
Analysis
C57BL/6
G
PLX3397+ - / + FTY720
vs.
PLX3397- food
D7
Analysis
C57BL/6
F
pLNs
mLNs
Spl.
Time (Days)
Ly-6C- CD44hi
Ly-6C+ CD44hi
CD44lo
H
Abs. Numb. of Ly-6C- CD44hi γδ T cells
Ctrl.
PLX3397
PLX3397 + FTY720

Figure 3

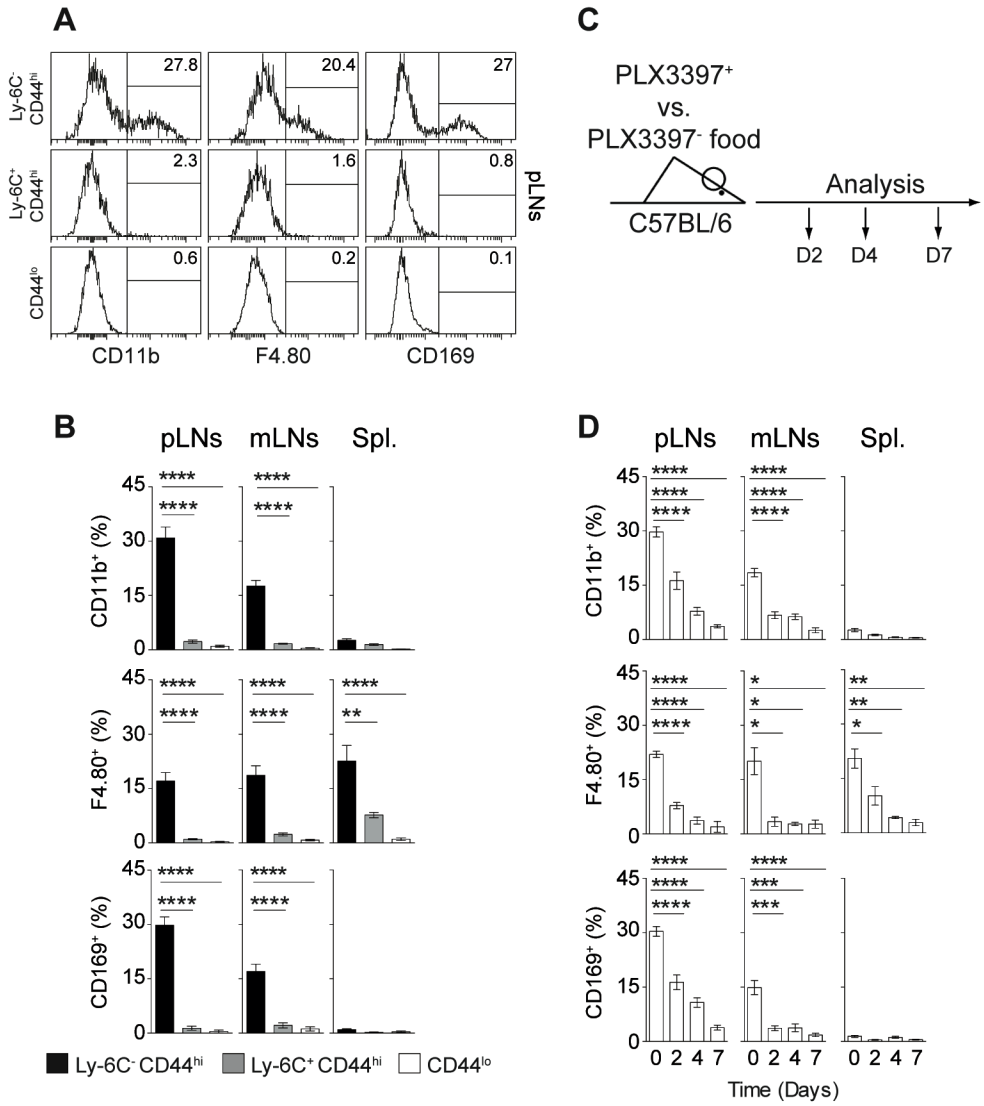
A
Ly-6C⁻ CD44ʰⁱ
Ly-6C⁺ CD44ʰⁱ
CD44ˡᵒ
27.8
20.4
27
2.3
1.6
0.8
0.6
0.2
0.1
pLNs
CD11b
F4.80
CD169
C
PLX3397⁺
vs.
PLX3397⁻ food
C57BL/6
Analysis
D2
D4
D7
B
pLNs
mLNs
Spl.
CD11b⁺ (%)
F4.80⁺ (%)
CD169⁺ (%)
Ly-6C⁻ CD44ʰⁱ
Ly-6C⁺ CD44ʰⁱ
CD44ˡᵒ
D
Time (Days)

Figure 4

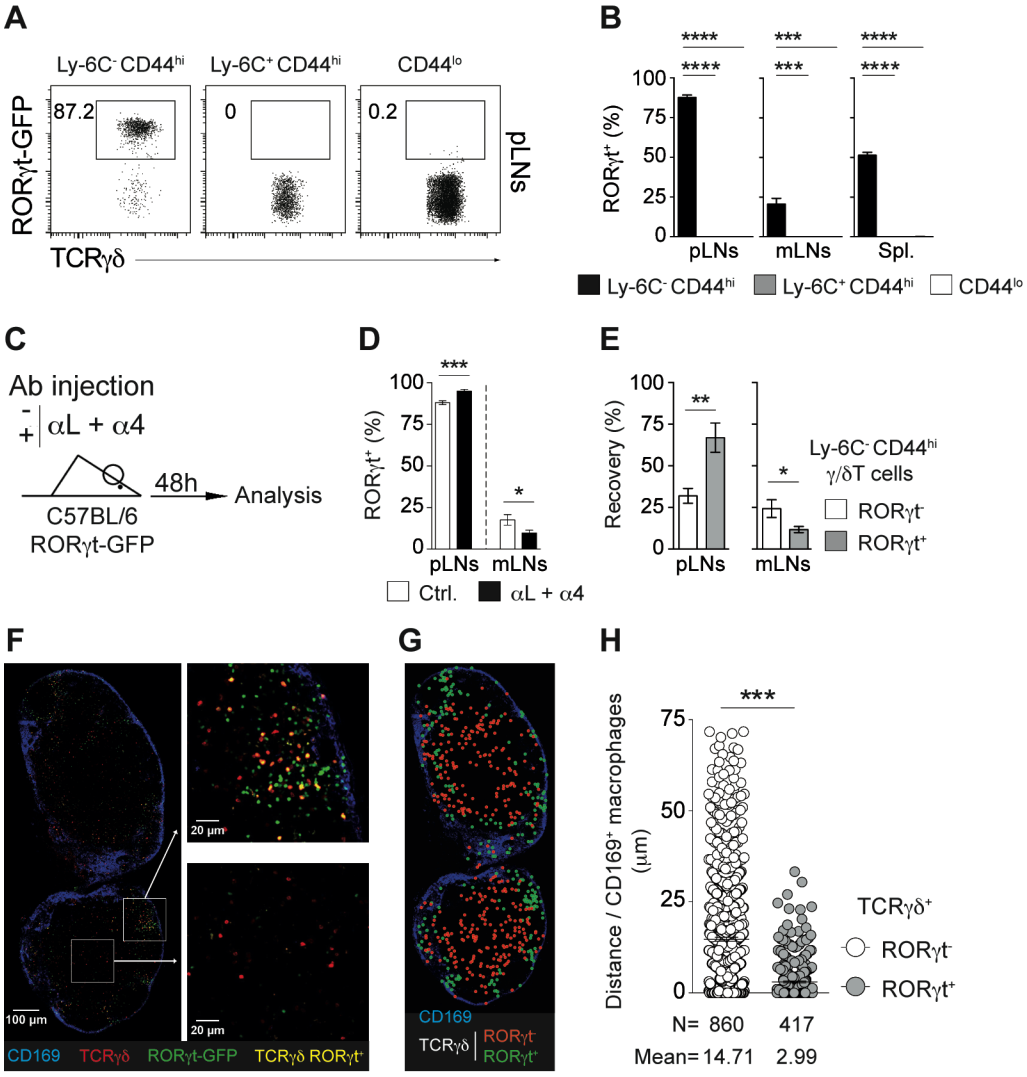
A
Ly-6C⁻ CD44hi
Ly-6C⁺ CD44hi
CD44lo
87.2
0
0.2
RORγt-GFP
TCRγδ
pLNs
B
RORγt⁺ (%)
pLNs
mLNs
Spl.
Ly-6C⁻ CD44hi
Ly-6C⁺ CD44hi
CD44lo
C
Ab injection
+ -
αL + α4
48h
Analysis
C57BL/6
RORγt-GFP
D
RORγt⁺ (%)
pLNs
mLNs
Ctrl.
αL + α4
E
Recovery (%)
Ly-6C⁻ CD44hi
γ/δT cells
RORγt⁻
RORγt⁺
F
100 µm
20 µm
CD169
TCRγδ
RORγt-GFP
TCRγδ RORγt⁺
G
CD169
TCRγδ
RORγt⁻
RORγt⁺
H
Distance / CD169⁺ macrophages (µm)
TCRγδ⁺
RORγt⁻
RORγt⁺
N= 860 417
Mean= 14.71 2.99
I
LPS injection
C57BL/6
RORγt-GFP
3h
Brefeldin A
2h
Analysis
J
pLNs
mLNs
Spl.
IL-17⁺ (%)
IFNγ⁺ (%)
Ctrl.
LPS
K
pLNs
mLNs
Spl.
IL-17⁺ (%)
IFNγ⁺ (%)
RORγt⁻
RORγt⁺

Figure 5